



Review

Thermal conductivity of carbon-based nanomaterials: Deep understanding of the structural effects

Yangsu Xie^{a,1}, Xinwei Wang^{b,*,2}

^a College of Chemistry and Environmental Engineering, Shenzhen University, Shenzhen 518055, Guangdong, PR China

^b Department of Mechanical Engineering, 271 Applied Science Complex II, 1915 Scholl Road, Iowa State University, Ames, IA 50011, USA



ARTICLE INFO

Keywords:

Thermal conductivity
Thermal reffusivity
Structure thermal domain size
Carbon-based nanomaterials
Phonons and electrons
Structure scattering
Anisotropic temperatures
Anisotropic specific heat

ABSTRACT

The thermal conductivity of carbon-based nanomaterials (e.g. carbon nanotubes, graphene, graphene aerogels, and carbon fibers) is a physical property of great scientific and engineering importance. Thermal conductivity tailoring via structure engineering is widely conducted to meet the requirement of different applications. Traditionally, the thermal conductivity–temperature relation is used to analyze the structural effect but this relation is extremely affected by effect of temperature-dependence of specific heat. In this paper, detailed review and discussions are provided on the thermal reffusivity theory to analyze the structural effects on thermal conductivity. For the first time, the thermal reffusivity-temperature trend in fact uncovers very strong structural degrading with reduced temperature for various carbon-based nanomaterials. The residual thermal reffusivity at the 0 K limit can be used to directly calculate the structure thermal domain (STD) size, a size like that determined by x-ray diffraction, but reflects phonon scattering. For amorphous carbon materials or nanomaterials that could not induce sufficient x-ray scattering, the STD size probably provides the only available physical domain size for structure analysis. Different from many isotropic and anisotropic materials, carbon-based materials (e.g. graphite, graphene, and graphene paper) have Van der Waals bonds in the c-axis direction and covalent bonds in the a-axis direction. This results in two different kinds of phonons whose specific heat, phonon velocity, and mean free path are completely different. A physical model is proposed to introduce the anisotropic specific heat and temperature concept, and to interpret the extremely long phonon mean free path despite the very low thermal conductivity in the c-axis direction. This model also can be applied to other similar anisotropic materials that feature Van der Waals and covalent bonds in different directions.

1. Introduction

Due to the intriguing properties of graphene and carbon nanotube (CNT), such as high electrical [1,2] and thermal conductivities [3], large specific surface areas, and high mechanical strength to weight ratios [4], graphite, graphene and CNT based nanomaterials, including carbon-based foams, aerogels, fibers, bundles, and mates, form a class of extremely promising materials for broad applications. Potential applications in electronics, thermal management [5], thermal electrical materials [6], photo-thermal conversion [7], and sensors [8–10] etc. have been widely reported. Also graphite and carbon-based composite materials have been widely applied in nuclear power plants for enhanced radiation tolerance and wonderful thermal conductivity [11,12]. Among these exceptional properties, the thermal conductivity is a critical property that determines the thermal response of materials

or devices to thermal loading. Various carbon-based materials, ranging from one-dimensional carbon nanotubes and fibers, two-dimensional films, to three-dimensional carbon composites (such as graphene foams, graphene aerogels, and graphene arrays) have been extensively studied for applications in thermal interface materials [13–16]. In addition, biomaterials such as chitosan and nanocellulose have recently emerged as promising candidates in thermal management [17,18]. Understanding the underlying physics responsible for the thermal conductivity of carbon-based nanomaterials is of significant importance for both fundamental study and applications.

Thermal conductivities as high as 1600–4000 W/m·K have been reported for single-layered graphene [19,20] and 2000–3500 W/m·K for single-walled carbon nanotubes (SWCNT) [21–23], far exceeding that of copper or gold. Nevertheless, when composited into bulk materials with nanostructures, like foams, aerogels, bundles, mats, or

* Corresponding author.

E-mail address: xwang3@iastate.edu (X. Wang).

¹ ORCID: 0000-0001-7731-1876

² ORCID: 0000-0002-9373-3750

fibers, the thermal conductivity is significantly hindered by several factors. First, the structural defects and impurities are inevitably brought into the structure during large scale production, which provide significant scattering sites for phonons. Defects including Stone–Wales defect, vacancies, functionalized groups, and charged impurities, etc., are difficult to interpret in detail. Research on the defects effect on thermal transport is vibrant in recent years. Second, among the basic units for forming these composite materials, weak interactions mainly including Van der Waals force and hydrogen bonds are responsible for the interconnection. This leads to very high thermal contact resistance at interfaces, which results in significant thermal conductivity reduction by several orders of magnitude. For graphene or CNTs based foams, bundles and fibers, the thermal conductivities were reported to be in a range of 15–79 W/m·K at room temperature [24–28]. For graphene aerogels with an ultralow density, the thermal conductivity can even be as low as 15 mW/m·K in air [29] and 4.7–5.9 mW/m·K in vacuum [30], which are very promising as advanced thermal insulating materials. Under thermal expansion/ shrinkage or mechanical strain, the energy transport mechanisms can be more complicated.

Furthermore, graphite, multi-walled CNTs, and multi-layered graphene have strong anisotropic structure. Covalent bonding exists in the in-plane direction, which facilitates fast phonon propagation; while along the out-of-plane direction, only the weak Van der Waals force is responsible for the inter-layer bonding. The energy coupling between interlayer carbon atoms through the Van der Waals force is much weaker than that through covalent bonding [31,32]. This results in strong anisotropic electrical and thermal transport properties. For graphite, the thermal conductivity in the out-of-plane direction has been reported to be only 5.7–6.8 W/m·K [33,34], which is two to three orders of magnitude lower than that of the in-plane direction. In anisotropic carbon-based nanostructures, the energy transport becomes more complicated than isotropic materials or anisotropic materials but with the similar chemical bonds. This structural complexity significantly hinders scientific understanding and engineering control of energy transport in carbon-based nanostructured materials.

To achieve accurate characterization of the thermal diffusivity and thermal conductivity of carbon materials, advanced thermal characterization techniques with unique capacity have been developed for specific carbon geometry or nanostructures. For carbon nanostructures in fiber or film morphology, the transient electrothermal (TET) technique was developed by our group for one-dimensional thermal characterization of thermal diffusivity, thermal conductivity, and specific heat [35]. For carbon nanostructures of extremely high/small electrical resistance, the TET technique is difficult to use. The transient photo-electro-thermal (TPET) technique can be used instead [36]. To measure fibers with very short thermal relaxation time, the pulsed laser thermal relaxation (PLTR) technique was developed for such purpose [37]. For highly anisotropic carbon nanostructures, both the in-plane and out-of-plane thermal diffusivity can be characterized by using PLTRII technique [38]. To characterize the thermal conductivity of 2D materials including suspended or supported graphene, the micro-Raman technique has been widely employed. Both time-domain differential Raman (TD-Raman) [39,40] and frequency-resolved Raman (FR-Raman) techniques [41] have unique advantages to measure the thermal diffusivity of 2D materials in a nonintrusive way. By using the recently developed energy transport state (five states in total)-resolved Raman (ET-Raman) [42–44], the thermal conductivity, the interface thermal resistance with substrate, and hot carrier diffusion coefficient/mobility can be determined simultaneously with sound accuracy. Details of the thermal characterization techniques developed by our group for carbon nanostructures have been reviewed in our previous work [45].

Challenges in developing carbon-based thermal interface materials include reducing the overall thermal resistance, improving the electrical insulation ability, lowering the cost for large-scale fabrication, as well as ensuring the endurance and reliability for practical applications [13–16]. Our goal of this review is to provide a deep insight into the

physics of energy transport in carbon-based nano-materials, rather than to provide a comprehensive review of the past work on structural effects on energy transport in these nanomaterials. The physical models reviewed in this work provide an in-depth understanding of thermal transport mechanisms in carbon nanostructures, which are essential to stimulate future research in overcoming the limitations which remain in structure design, fabrication, and thermal resistance reduction for highly efficient thermal interface materials. The content of paper is divided into four sections. First, the temperature effect on energy transport is introduced, which is mainly influenced by phonon population or structural change. Second, the effect of structure improvement on enhancing energy transport is reviewed. Third, the energy transport along the Van der Waals bond direction is discussed based on an anisotropic specific heat and temperature model. Finally, we discuss the energy transport sustained by combined Van der Waals force and covalent bonds.

2. Temperature effect on energy transport: phonon population and structural change

Temperature has significant effects on the energy transport in carbon-based nanomaterials. For most carbon-based nanomaterials, phonons are the main heat carriers. The electrons' contribution to thermal conductivity is insignificant based on the Wiedemann-Franz law. A phonon is a quantum mechanical description of lattice vibrational motion [46]. From kinetic theory of gases, the thermal conductivity (k) resulted from phonon propagation is $k = C\nu\Lambda/3$ for isotropic materials, where C is the heat capacity per unit volume, ν is the average velocity of phonons, and Λ is the mean free path of phonons. During phonon propagation, phonons could encounter scattering from not only phonons, but also from the scattering centers in the structure, such as impurities, lattice defects, and grain boundaries, etc. Historically, researchers have analyzed the phonon scattering mechanisms from the k - T profiles [47,48]. Fig. 1(a) shows the measured thermal conductivity of three pyrolytic graphite materials [33,49,50]. The peak of k - T profiles divides temperature into two regimes. At high temperature above the peak- k temperature, Λ is mainly limited by the phonon-phonon scattering. Nevertheless, at low temperatures below the peak- k temperature, the structure-induced scattering is the dominant limit and the Λ value becomes a constant at sufficiently low temperatures, which is determined by the microstructure of the material. Thus, at low temperatures, the k - T profiles usually vary as C - T profiles. However, the temperature dependent behavior of heat capacity C is very complex, which is also closely related to the microstructure of carbon materials. Furthermore, experimentally measuring the heat capacity of carbon nanostructures at low temperatures is very challenging. This makes it difficult to directly evaluate the phonon scattering mechanisms based on k - T profiles.

In recent years, Wang's group has developed a theory of thermal reffusivity to directly analyze the phonon scattering intensity [51,52]. The 'thermal reffusivity' of semiconductors and nonconductors, whose main heat carriers are phonons, was first defined in Xu et al.'s work as [53]:

$$\Theta = 1/\alpha, \quad (1)$$

where α is the thermal diffusivity. Combining with the kinetic theory of gases for thermal conductivity, the thermal reffusivity can be expressed as $\Theta = 3/(\nu\Lambda)$, where ν and Λ are the velocity and mean free path of phonons. According to Matthiessen's rule, the contribution from different scattering mechanisms can be linearly summed up to obtain the total scattering intensity. Therefore, the thermal reffusivity can be further expressed by phonon relaxation time as:

$$\Theta = \frac{3}{\nu^2} \left(\tau_{\text{phonon}}^{-1} + \tau_{\text{structure}}^{-1} \right) \quad (2)$$

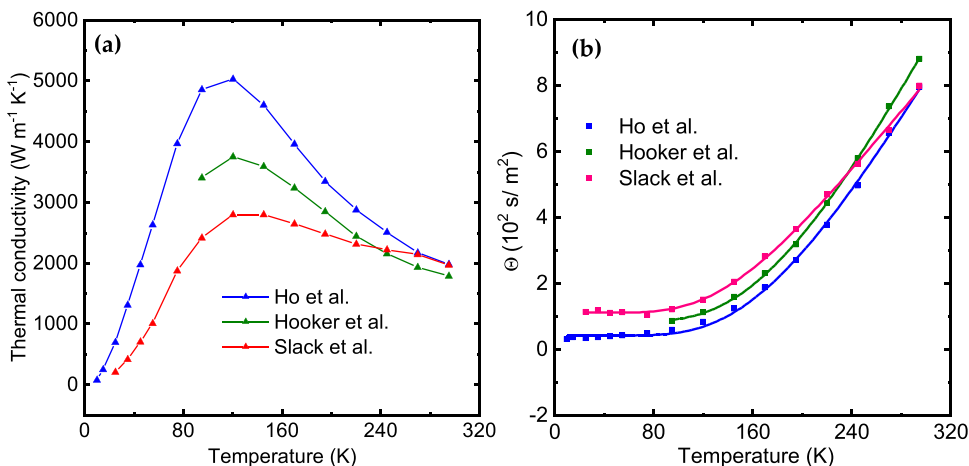


Fig. 1. (a) The thermal conductivity and (b) thermal reffusivity of pyrolytic graphite [33,49,50]. The solid lines in (b) are the theoretical fitting of the data based on the thermal reffusivity model expressed in Eq. (3). The residual value of Θ at 0 K limit is taken as the residual thermal reffusivity (Θ_0) [51]. (Reproduced from Ref. [51] with permission from the Royal Society of Chemistry.).

Here τ_{phonon} is the phonon relaxation time from Umklapp phonon-phonon scattering (U-scattering), and $\tau_{\text{structure}}$ is the phonon relaxation time from structure-induced scattering, which includes the scattering from lattice defects, chemical impurities, and grain boundaries, etc. The minimum energy for phonons to participate in the U-scattering process needs to be in the order of $k_B\theta/2$, in which k_B is the Boltzmann's constant and θ is the Debye temperature. As a result, the phonon population participating in U-scattering follows a temperature (T) dependent behavior of $e^{-\theta/2T}$ (the constant can vary from 2 to 2.5) according to the Boltzmann factor [54]. In the temperature range much lower than θ , the $\tau_{\text{phonon}}^{-1}$ value also presents a temperature dependence as $\sim e^{-\theta/2T}$. On the other hand, $\tau_{\text{structure}}$ has a weak temperature dependence. For carbon-based materials, the phonon velocity can be assumed to be independent of temperature. Then Θ is expressed as:

$$\Theta = \Theta_0 + C \times e^{-\theta/2T} \quad (3)$$

Eq. (3) is the thermal reffusivity model for semi-conductors and insulators. It is clear from this equation that the Θ value of a material is expected to decrease as temperature goes down and approach a constant Θ_0 at the 0 K limit. Θ_0 is the residual thermal reffusivity, which directly reflects the structure-induced phonon scattering intensity. The Θ_0 value is determined by the defect level (structure domain size) of the material. In addition, the trend of Θ - T curves is related to the Debye temperature θ , which is the highest temperature of a crystal that can be achieved by single normal vibration. It is a useful proxy for crystal rigidity, which is related to the strength of inner structural connectivity [55]. By fitting the experimental data with the thermal reffusivity model in Eq. (3), the value of Θ_0 and θ can be extracted. The structure-induced phonon scattering intensity can be decoupled from the phonon population effect.

Fig. 1(b) shows the experimentally measured thermal reffusivity of graphite (calculated from the data of literatures) at low temperatures. As temperature decreases, Θ of the three pyrolytic graphite materials goes down, and finally reaches constant values. This Θ - T behavior is consistent with that predicted by the thermal reffusivity model introduced above. As shown in Fig. 1, the experimentally measured data can be fitted with good accuracy by the thermal reffusivity model expressed in Eq. (3). As temperature approaches the 0 K limit, the thermal reffusivity of the three pyrolytic graphite materials goes to constant values. From the three thermal reffusivity data from Ho et al., [49], Hoover et al. and Slack et al., [33], the Θ_0 values were determined to be 43.3, 84.7 and 112.1 s/m² respectively. Their Θ value at room temperature were 795.4 s/m², 881.8 s/m² and 800.0 s/m² respectively. As a result, Θ_0 takes 5%, 9.6% and 14% of the Θ at room temperature. This indicates that the defect density in those pyrolytic graphite samples is very low. Furthermore, the Debye temperature was obtained by fitting the experimental data based on the thermal reffusivity model in Eq. (3).

θ was determined to be 1349 K (Ho et al [49]), 1381 K (Hoover et al.) and 1133 K (Slack et al [33]), respectively, which are very close to the Debye temperature of ZA mode (1120 K). This reflects the dominant role of the ZA mode phonons in heat conduction in those pyrolytic graphite samples [51]. Similar behavior has also been observed in graphene foams grown by the chemical vapor deposition method [51], carbon nanocoils [56], and high purity graphene films [57], etc.

With the development and application of carbon-based materials, novel carbon materials have been designed and fabricated in recent years, such as graphene foam, graphene aerogel, carbon fibers, and graphene fibers, etc. However, some of these carbon materials show Θ - T behaviors very different from what the thermal reffusivity model predicts. The reason is the dominant effect of structure defects-induced phonon scattering in the structure, which shows weak temperature dependence. Liu et al. studied the structure and thermal properties of lignin-based carbon micro-fibers (CF), which was produced by melt-spinning of pyrolytic lignin derived from red oak. Fig. 2(a) shows the experimentally measured thermal reffusivity against temperature. The thermal reffusivity only shows small decrease as temperature goes down from 300 K to around 125 K. In the temperature range of 125–10 K, the thermal reffusivity just fluctuates with a maximum/minimum ratio of only 1.43, indicating that phonons are dominantly scattered by structure defects in this temperature range [58]. This indicates very strong defects-induced phonon scattering in CF.

For carbon materials prepared by self-assembling methods, such as graphene aerogels, graphene fibers, and graphene films, the inner connection among the nanostructures are not through covalent bond. Instead, weak Van der Waals force is responsible for the interconnection among the nanostructures in these materials. As a result, the nano-interfaces among the nanostructures provide large amount of scattering sites for phonons during propagation. When temperature reduces, the thermal reffusivity of these materials just fluctuates or even goes up, rather than going down. This reflects the strong contact degrading at low temperatures. By analyzing the Θ - T trend the evolution of the interconnection and interfaces-induced phonon scattering can be attained. This cannot be discovered by simply analyzing thermal conductivity versus temperature data, where the specific heat effect overshadows the interfaces effect, and the thermal conductivity will go to zero when temperature goes to 0 K.

Fig. 2(b) and (c) show the experimentally measured thermal reffusivity of graphene aerogels (GA) synthesized by chemical reduction of graphene oxide solution [30] and partly reduced graphene oxide (PRGO) films synthesized by vacuum-assisted filtration [57], respectively. The Θ - T curves show an increasing behavior as temperature goes down. The negative temperature coefficient of Θ indicates that the structure-induced scattering intensity in these materials increases at low temperatures. In GA and PRGO films, the partly reduced graphene

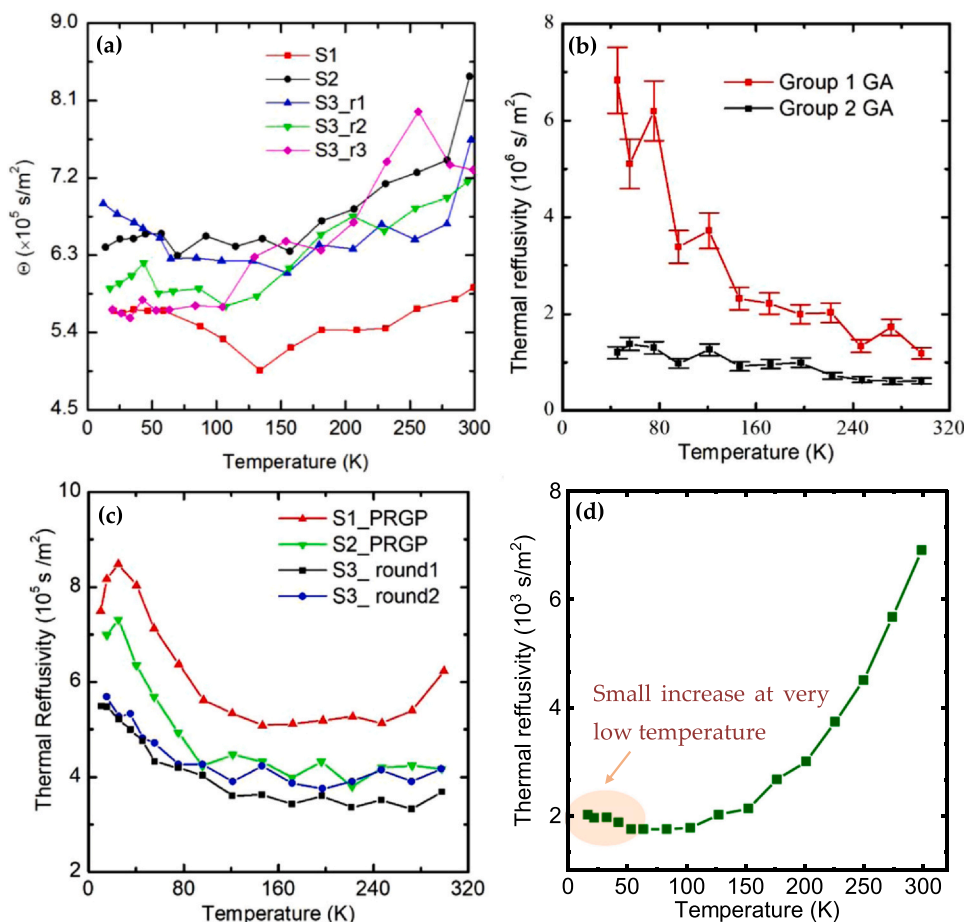


Fig. 2. The thermal reffusivity against temperature for several carbon-based materials where strong structural contact degrading at low temperatures dominates the energy transport at the microscale; (Reprinted from Ref. [58] with permission from Elsevier.) (b) graphene aerogels; (Reprinted from Ref. [30] with permission from Springer Nature.) (c) partly reduced graphene oxide (PRGO) films synthesized by vacuum-assisted filtration; (Reproduced from Ref. [57] permission from the Royal Society of Chemistry.) (d) graphene foam synthesized by chemical vapor deposition. (Reproduced from Ref. [51] with permission from the Royal Society of Chemistry.)

oxide flakes are the basic building units, which are assembled together mainly through the weak Van der Waals force. At low temperatures, the interconnection among nanostructures in these materials is deteriorated due to thermal expansion or shrinkage of the nanostructures. As a result, the interfaces provide stronger scattering intensity for phonons, which causes Θ to rise with the reduced temperature. These results uncover significant thermal contact resistance among neighboring nanostructures and interface-mediated thermal transport in GA and PRGO films.

Fig. 2(d) presents the Θ - T data of graphene foam fabricated by chemical vapor deposition [51]. Graphene foam has a continuous nanostructure, where the graphene flakes are seamlessly inter-connected. From 295–50 K, the Θ - T curve shows a decreasing trend as temperature goes down, which indicates the dominant role of U-scattering in this temperature range. However, at very low temperatures (below 50 K), a small rise of Θ can be observed. This indicates structure degrading, which makes the thermal reffusivity goes up at very low temperatures. Note such structure degrading or breakdown is impossible to observe in thermal conductivity-temperature curves.

It should be noted that the different thermal reffusivity-temperature trends are resulted from the different defect densities and atomic bond strength in the materials, which cannot be simply determined by the dimension of carbon nanomaterials. For the same type of nanomaterial, the defect level can vary if they are prepared by different methods. As a result, their thermal reffusivity-temperature curves can deviate significantly. Thus it is difficult to directly categorize the applicability of thermal reffusivity models. However, by using the Θ - T curves, we can identify the defect level and have a better understanding of the structure bond strength in carbon nanomaterials. We summarize the thermal reffusivity-temperature trends and the corresponding structure features of carbon nanomaterials in Table 1.

3. Energy transport improvement by structural improvement: the ultimate factor

The ultra-high intrinsic thermal conductivity of graphene and carbon nanotubes makes carbon-based materials promising candidates for thermal management. Bulk carbon materials have been developed to meet the requirements of application, such as graphene films, carbon nanotube arrays, and carbon fibers, etc. However, large-scale fabrication always yield carbon-based materials with contaminants and lattice defects, which significantly affect their thermal and electrical conductivity. To boost the energy transport ability, methods including thermal annealing, mechanical processing, chemical reduction, and laser processing, etc. have been proposed to improve the structural purity or alignment. Thermal annealing is the most widely used method for improving the thermal conductivity of carbon-based materials. Mechanical stretching also has been reported for thermal conductivity enhancement of carbon nanotube fibers, which is resulted from the better alignment and improvement of thermal contact between carbon nanotubes [59]. Chemical reduction has also been widely used for its significant effect in reduction of oxygen-containing functional groups and improvement of bonding strength [60]. In addition, our recent work reveals the mechanisms of photoreduction: immediate and fast photochemical removal of oxygen functional groups, followed by laser heating that facilitates thermal rearrangement of GO sheets towards better graphitization [61].

By studying the Θ - T curves, it can help give good insights into the complex mechanisms associated with the energy transport improvement, which cannot be attained by simply studying the k - T curves. On the one hand, the residual value of thermal reffusivity at 0 K limit (Θ_0) can be used to study the structure domain size, which is determined by the mean free path of acoustic phonons at 0 K limit (Λ) according to the following equation:

Table 1

The thermal reffusivity-temperature trends and the corresponding structure features.

Structure features	Θ - T trend	Typical carbon materials
Most crystalline carbon materials	Θ decreases as temperature reduces and approaches a constant value Θ_0	Graphite, carbon nanotube, CVD grown graphene foam, high purity graphene film
High defects density	Θ shows a weak temperature dependence	Carbon fibers, graphene oxide films
Weak inner structural connectivity	Θ increases slightly as temperature goes down	Graphene aerogel, partly reduced graphene oxide films

$$\Lambda = \frac{3}{\Theta_0 v} \quad (4)$$

where Λ is the phonon mean free path caused by phonon scattering at grain boundaries and defects. The Λ size is a measure of structure defects, which is comparable to the real crystallite size. It is not precisely the same as that measured from x-ray diffraction (XRD) spectroscopy. The XRD spectroscopy provides information about the crystallite size in a specified direction; while the Λ size is a result from the phonon scattering effect from all the lattice directions. For materials whose crystallite sizes are difficult to obtain by XRD, such as amorphous materials (polymers and organic materials), materials with very large crystallite sizes, or nanomaterials having very small scattering cross-section, Λ provides an excellent alternative and complement for estimating the structure domain sizes.

Furthermore, the trend of the Θ - T curve is determined by the Debye temperature of the test-material. The Debye temperature θ is the temperature of a crystal's highest normal mode of vibration, which is associated with the interatomic bonding force. If the interatomic bonding is improved, the corresponding θ is expected to become higher. Therefore, by studying the Θ - T curve, the structure domain sizes and interatomic bonding strength of materials can be analyzed, which provides a more advanced way to understanding the structure improvement. Therefore, from the analysis of Θ - T curves, if the Θ_0 value is reduced, it indicates that the structural defects are reduced and the structure domain sizes are increased. If the slope of Θ - T curves is higher (or lower), it indicates the strength of inner structural connectivity becomes stronger (or weaker) according to the thermal reffusivity model in Eq. (3).

The thermal reffusivity model has been used for characterizing the structural evolution of carbon fibers and graphene fibers during thermal annealing. Oxygen-containing functional groups in sp^3 carbon bonds can be removed by thermal annealing treatment, during which the graphitic grain growth is also promoted, leading to increase of the structure domain size and enhancement of thermal conductivity. Liu et al. studied the annealing effects on the thermal properties as well as micro-structures of lignin-based microscale carbon fibers [58]. Fig. 3(a) shows the measured thermal conductivity, which shows a 24~44% increase at room temperature after thermal annealing. The k - T curves are similar for both pre-annealed and post-annealed samples. However, from the k - T curves, very little knowledge can be obtained about how the structure improvement contributes to phonon transport. To have a better understanding of the underlying mechanism for the thermal conductivity enhancement, the Θ - T curves were studied. The Θ - T curves of the pre-annealed and post-annealed samples show parallel trend as temperature goes down [Fig. 3(b)], indicating that the effect of thermal annealing treatment on the Debye temperature is very weak. This demonstrates that the interatomic bonding force of lignin-based microscale carbon fibers was not significantly changed by thermal annealing. Instead, the Θ_0 value was significantly reduced after thermal annealing, which decreased from 7.13×10^5 to 4.11×10^5 s/m², and from 8.10×10^5 to 6.31×10^5 s/m², for the two samples, respectively. As a result, the effective phonon mean free paths of the two CF samples were found increased by 72% and 28%, respectively. From the analysis of Θ - T curves, it is evident that the thermal annealing improved the thermal transport by reducing the structural defects and increasing the structure domain sizes, rather than enhancing the interatomic bonding of lignin-based microscale carbon fibers.

The Θ - T curves of graphene microfibers were studied by Lin et al. in order to better understand the mechanism behind the improvement of thermal conductivity by thermal annealing [62]. Fig. 3(c) and (d) show the Θ - T curves of the two graphene microfibers. The experimental data was fitted based on the thermal reffusivity model in Eq. (3). It was found that the structure domain size was increased significantly by thermal annealing. Additionally, the Θ - T curves for pre-annealed and post-annealed samples also show very parallel trend, which indicates that the interatomic bonding was not significantly improved by thermal annealing.

4. Energy transport along the Van der Waals bond direction: anisotropic specific heat and temperature

As discussed above, for phonon transport along the in-plane direction (termed a-axis) of carbon-based structures, the thermal reffusivity can be taken as the inverse of the thermal diffusivity. However, this scenario will become completely different and more complicated for the phonon transport along the cross-plane direction, here termed c-axis. Fig. 4(a) shows the structure of graphene paper (GP) and that the heat conduction in the c-axis in fact is across the basal planes. This also holds true for graphite and other similar anisotropic materials, like MoS₂, WS₂, and so on. As shown in Fig. 4(b), within a basal plane, atoms are bonded together via covalent bonds, which sustains the in-plane thermal conductivity. The related phonons are termed "a-phonon" here. However, the thermal transport along the c-axis is sustained by the Van der Waals bonds among atoms, which is much weaker than the in-plane covalent interaction. The pertaining atomic movements and interactions are related to the phonons termed "c-phonon" here. As a result, the c-axis thermal conductivity is 2–3 orders of magnitude smaller than that of in-plane, as clearly shown in Fig. 5. For the thermal conductivity of a-phonons and c-phonons, at present no study has been reported yet on their relation. It is expected any defect level within the material will affect both thermal conductivities, but could be to different extent. This depends on how this defect is distributed in space: whether it is more like c-axis defect or a-axis defect. For instance, if the material has more small grains in the basal planes, the a-phonon thermal conductivity will be reduced significantly. These a-plane grains will have little effect on the c-axis atomic interaction, so the c-phonon thermal conductivity will be reduced insignificantly.

As the in-plane covalent bond atomic interactions are independent of the c-axis Van der Waals interactions, the a-phonon energy cannot be directly transported along the c-axis. The a-phonon energy has to be transferred to the c-phonons first, then is transported along the c-axis. This mechanism can be described using an anisotropic specific heat and temperature model as below:

$$\frac{\partial C_c T_c}{\partial t} = k_c \frac{\partial^2 T_c}{\partial z^2} - G \cdot (T_c - T_a) \quad (5a)$$

$$\frac{\partial C_a T_a}{\partial t} = k_a \left(\frac{\partial^2 T_a}{\partial x^2} + \frac{\partial^2 T_a}{\partial y^2} \right)_a + G \cdot (T_c - T_a) \quad (5b)$$

Here T_a and T_c are the temperatures of a-phonons and c-phonons, respectively. G is the energy coupling factor between them. C_a and C_c are the volumetric specific heat of a-phonons and c-phonons, respectively. In the above equations, the z coordinate is along the c-axis. T_a

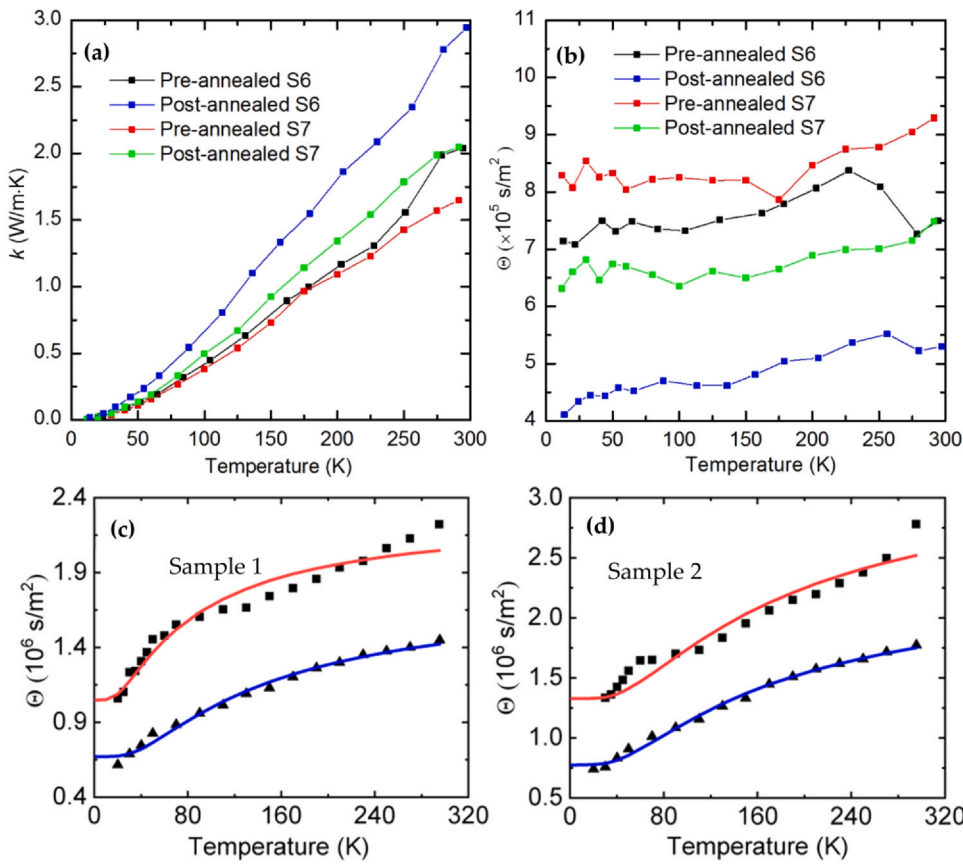


Fig. 3. The comparison of thermal reffivity against temperature before and after thermal annealing for understanding the structure improvement effect. (a) Thermal conductivity and (b) thermal reffivity for the pre-annealed and post-annealed lignin-based microscale carbonfibers. (Reprinted from Ref. [58] with permission from Elsevier.) (c) and (d) The thermal reffivity of two graphene microfibers before and after annealing. The red line is the fitting curve of the data before annealing, and the blue line is the fitting curve of the data after annealing. (Reprinted from Ref. [62] with permission from Elsevier.)

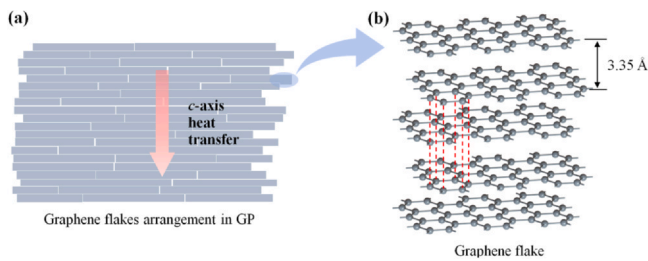


Fig. 4. Schematic of energy transport along the Van der Waals bond direction in graphene paper. (a) The c-axis thermal transport across the graphene flakes in a graphene paper, (b) details of Van der Waals interactions among atoms in the c-axis direction. (Reprinted from Ref. [63] with permission from Elsevier.)

and T_c are in equilibrium for most of the time, considering the very fast energy exchange among C_a and C_c . However, it should be noted that they are separately involved in heat conduction in the a-axis and c-axis. So for sole heat conduction along the c-axis, there will be no temperature gradient in the a-axis direction (x and y coordinates). But even under such scenario, for very fast transient heat conduction, there will be thermal nonequilibrium between a-phonons and c-phonons, and the anisotropic temperature model has to be considered. Based on this physical model, the c-axis thermal reffivity should be defined as $\Theta_c = C_c/k_c$ by using the volumetric specific heat of c-phonons instead of all the phonons. This is different from the inverse of the normal thermal diffusivity that uses the overall phonon specific heat.

Although theoretically it is straightforward to determine the phonon dispersion relations for a-phonons and c-phonons, no work has been

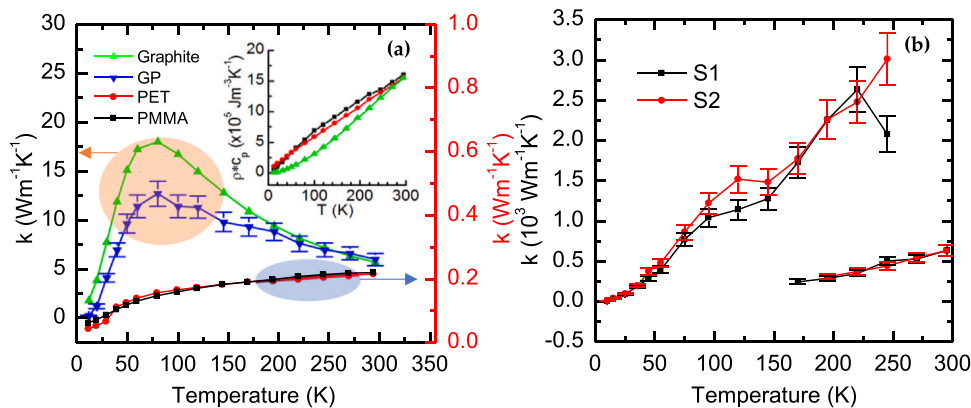


Fig. 5. The anisotropic thermal conductivity of graphene paper. (a) The c-axis thermal conductivity of graphene paper and graphite, (b) the a-axis thermal conductivity of graphene paper. (Reprinted from Ref. [63] with permission from Elsevier.)

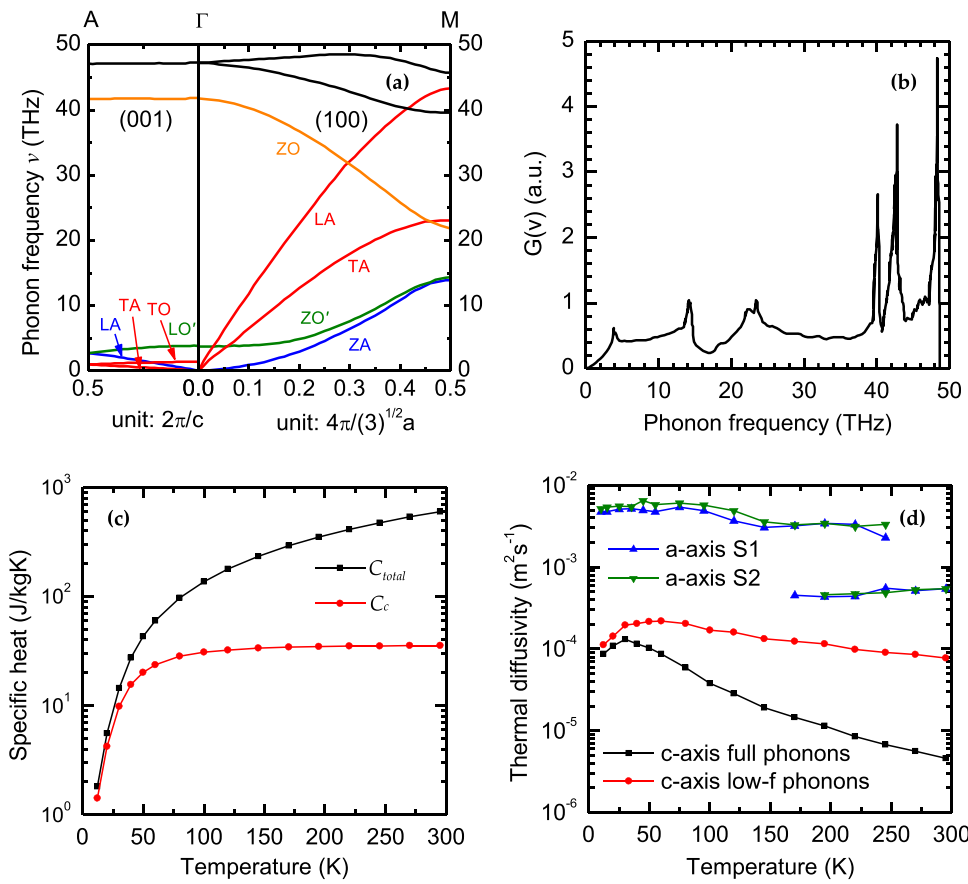


Fig. 6. The dispersion relations, specific heats and thermal diffusivity calculations for a-phonons and c-phonons of graphite. (a) Dispersion relation for a-phonons and c-phonons, (b) density of state of phonons, (c) specific heat of all phonons (C_{total}) and C_c , and (d) thermal diffusivity calculation based on different phonon specific heat consideration. (Reprinted from Ref. [63] with permission from Elsevier.)

done to distinguish their specific heats and temperatures. a-phonons in fact only transport along the a-axis direction and c-phonons only along the c-axis direction. So their velocities are also very different. Fig. 6 shows the dispersion relations for a-phonons and c-phonons, their specific heats and thermal diffusivity calculations [63].

As shown in Fig. 6(a), the c-phonons have much lower velocities than a-phonons. Also for c-phonons, the TO and LO' branches of optical phonons have low frequencies, meaning they can be excited well even at room temperature. This is quite different from a-phonons. Fig. 6(b) shows the density of state of phonon branches in graphite. The calculation results of the specific heat is show in Fig. 6(c). From Fig. 6(c) it is evident that C_c is much smaller than the overall phonon specific heat

C_{total} . At room temperature, the calculation shows $C_{total}=601 \text{ Jkg}^{-1}\text{K}^{-1}$ and $C_c=35.7 \text{ Jkg}^{-1}\text{K}^{-1}$. Note this estimation still carries some uncertainties since at low frequencies, both a-phonons and c-phonons are hard to distinguish for their contributions to specific heat. A more rigorous way is via molecular dynamics (MD) simulation, which could distinguish the specific heat rigorously. Fig. 6(d) shows the calculation results of thermal diffusivity along the c-axis direction based on the c-phonon heat capacity and the total heat capacity. The measured thermal diffusivity along the in-plane direction is also presented for comparison. It can be seen that compared with the strong anisotropy of thermal conductivity shown in Fig. 5, the thermal diffusivity shows much smaller anisotropy (one order of magnitude smaller).

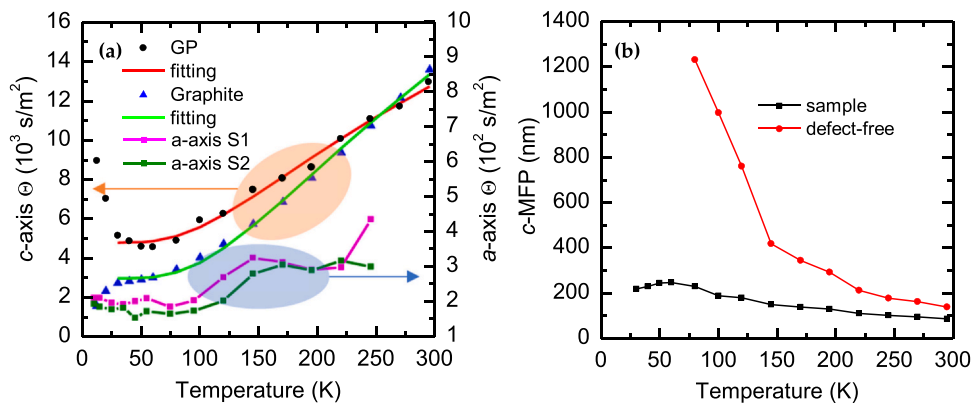


Fig. 7. Thermal reffusivity and mean free path calculation for phonons in the a-axis and c-axis directions considering the anisotropic specific heat for graphene paper. (a) Thermal reffusivities in the a-axis and c-axis directions. (b) Phonon mean free path of c-phonons. (Reprinted from Ref. [63] with permission from Elsevier.)

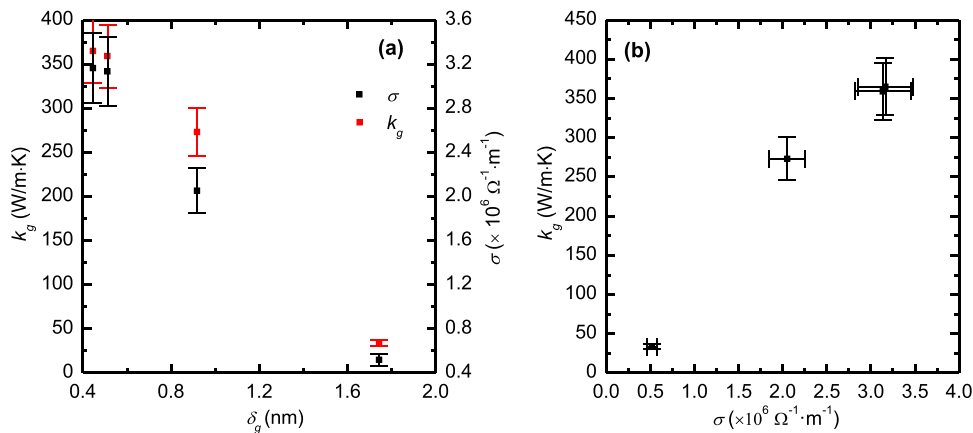


Fig. 8. The linear coherency between electrical and thermal conductivities of few-layered graphene on PMMA. (a) Variation of electrical and thermal conductivities of graphene against the its average thickness. (b) Linear coherency between electrical and thermal conductivities for the graphene samples. (Reproduced from Ref. [67] with permission from the Royal Society of Chemistry.)

The above anisotropic specific heat and temperature consideration becomes insignificant under slow heat conduction where the a-phonons and c-phonons quickly establish their thermal equilibrium with a characteristic time much smaller than the heat transfer characteristic time. However, for ultrafast heat conduction, e.g., when a material is under pico- or femto-second laser heating, this model needs to be considered rigorously.

Also when evaluating the structure thermal domain (STD) size in the c-axis direction, this model must be considered rigorously. Fig. 7 shows our past work on thermal reffusivity calculation in the a-axis and c-axis directions considering the anisotropic specific heats [63]. With such consideration and use of the c-phonon velocity, the STD size in the c-axis direction of graphene paper is found to be 234 nm. This size uncovers excellent structural order but is difficult to determine using XRD

since it exceeds the machine's limit. Also using the anisotropic specific heat theory, the phonon mean free path at room temperature is found to be 138 nm for defect-free GP. This is very close to that for graphite (146 nm) calculated by MD modeling. For graphite, based on the reported thermal conductivity, we calculated a mean free path of 165 nm based on the anisotropic specific heat model.

5. Energy transport sustained by combined Van der Waals and covalent bonds: coherency between phonon and electron conduction

As stated in the above section, the heat conduction in carbon-based materials in fact is sustained by two types of phonons: a-phonons and c-

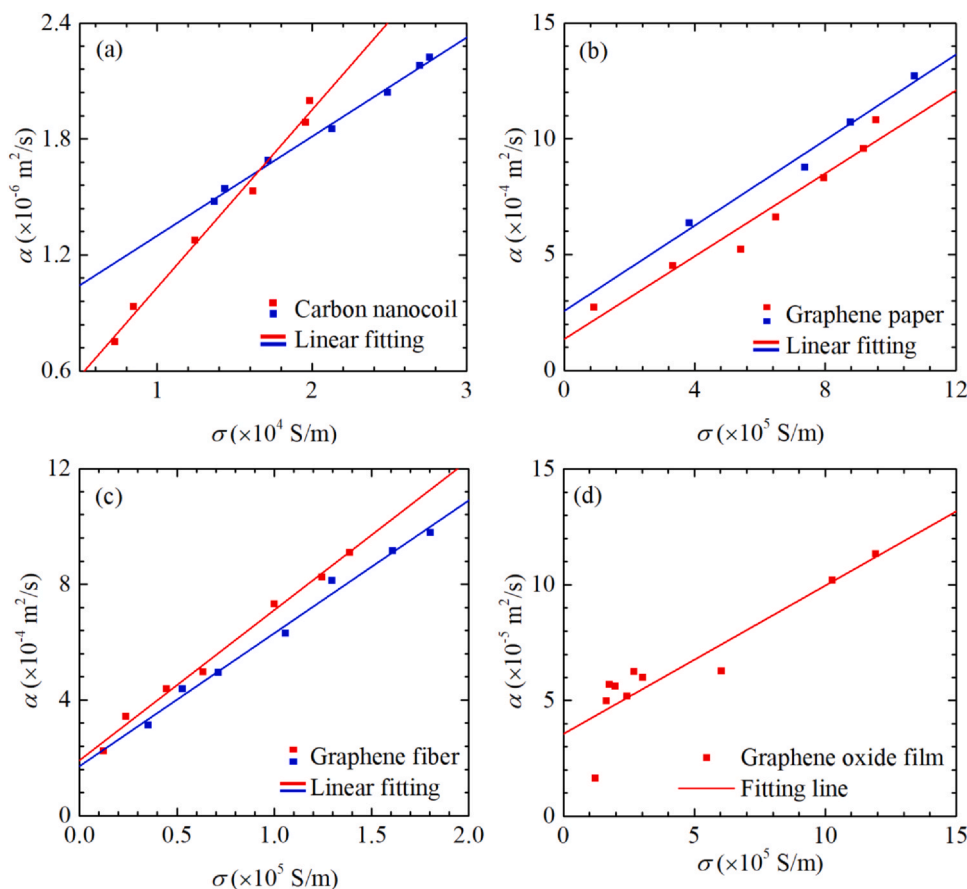


Fig. 9. The linear coherency between electrical conductivity and thermal diffusivity for (a) carbon nanocoils, (b) graphene paper, (c) graphene fiber, and (d) graphene oxide film. (Reprinted from Ref. [44] with permission from Elsevier.)

phonons, which are facilitated by different atomic bonds, and feature different velocity, specific heat, phonon dispersion relation, and phonon mean free path. This very different heat conduction mechanism in fact strongly affects the heat conduction in structured carbon materials, regardless of the structure order. In carbon-based micro/nanoscale and structured materials, the electric conductivity is sustained by electron transport, and such electron transport has negligible contribution to energy transport compared with that by phonons. However, it has been very well documented that in so many carbon-based materials, like carbon nanocoil, graphene, and carbon fibers, there is a linear relation between thermal conductivity and electrical conductivity [64–67]. Fig. 8 shows the excellent linear coherency between electrical and thermal conductivities of few-layered graphene on PMMA. This linear coherency holds true over a very large variation of the electrical and thermal conductivities, rather than simple linear approximation over a small change. The observed large thermal and electrical conductivity change with thickness [Fig. 8(a)] is attributed to the increased defect level in the sample when the chemical vapor deposition (CVD) grown thickness increases.

This intriguing phenomenon has been explained under the frame of phonon and electron scattering by defects. For instance, when the defect level is higher, both phonon and electron will experience stronger scattering, and their mean free path will be reduced, so as the thermal and electrical conductivities. For phonon transport, the defect level has negligible effect on the specific heat and phonon velocity, so it can be estimated as $k \propto l_p$, here k and l_p are the thermal conductivity and phonon mean free path. However, for electrons, its electrical conductivity (σ_e) is related to both electron mean free path (l_e) and density (n_e) as $\sigma_e = n_e e^2 \tau / m_e = n_e e^2 l_e / (m_e v_F)$ where n_e , e , τ , l_e , m_e , and v_F are the density, charge, relaxation time, mean free path, mass, and the Fermi velocity of electrons. Since carbon materials are semiconductive, its free electron density is not a constant. Instead, it is strongly affected by temperature and defect levels. Therefore when defect levels changes, n_e will also change. This, in fact complicates the theory based on coherent defect scattering of phonons and electrons.

The coherency between electrical and thermal conductivities, however, can be explained by the strongly anisotropic nature of electrical and thermal transport in carbon-based materials. As discussed above, the a-axis thermal conductivity of graphene and graphite materials is much higher than that of c-axis (2–3 orders of magnitude higher). This is also true for electrical conductivity. It has been discovered that graphite's a-axis electrical conductivity is much higher than that of the c-axis ($\sim 10^4$ times) [68]. Such almost insulative electrical and thermal conduction behavior in the c-axis direction will force electron and phonon transport to be always along the a-axis in carbon-based materials, regardless of the structure order. Therefore, the thermal and electrical conductivities of carbon-based structures can be expressed as

$$k = \gamma k_d + (1 - \gamma)k_g, \quad \sigma_e = \gamma \sigma_d + (1 - \gamma)\sigma_g \quad (6)$$

where γ is the volume fraction of defects. k_d , k_g are the thermal conductivity of defect and graphite-like structure, and σ_d , σ_g are the electrical conductivity of defect and graphite-like structure, respectively. The structure's a-axis electrical and thermal transport is sort of like following a link consisting of these structural grains. Fig. 9 summarizes the coherency between electrical conductivity and thermal diffusivity of many different micro/nanoscale structured carbon materials [66]. For each material, the volumetric specific heat is constant, so these figures indeed reflect the linear coherency between electrical and thermal conductivities.

6. Summary and outlooks

In this combined review and perspective, we outlined the theories and treatment about the structural effects on the phonon transport in carbon-based nanoscale and nanostructured materials. In contrast to the traditional way of using the thermal conductivity-temperature

curve to analyze the structural effects, the thermal reffusivity-temperature relation provides more advanced analysis and in-depth physics. The slope/trend and residual thermal reffusivity all reflect different aspects of structural effects. For a normal material whose structure not affected by temperature, its thermal reffusivity will go down with decreased temperature. However, for many nanostructured carbon materials, like graphene aerogel, carbon fiber, and graphene oxide films, the thermal reffusivity shows an increasing trend versus reduced temperature, uncovering strong structural degrading. Such physics is almost impossible to discover from the thermal conductivity-temperature analysis. The residual thermal reffusivity directly reflects the structure thermal domain size, which can be used to quantitatively assess the structural quality of carbon-based nanomaterials.

For the c-axis thermal transport, Van der Waals phonons sustains the heat conduction, and they have a specific heat different from that of in-plane phonons (a-phonons). The anisotropic specific heat and temperature model is critical for carbon-like materials whose anisotropic structure features both Van der Waals and covalent bonds. This is especially true and important for ultrafast energy transport and structure thermal domain size analysis. The thermal and electrical conductivities in the a-axis of carbon-based materials is a few orders of magnitude higher than those along the c-axis. Such ultra-anisotropy determines that in carbon structured materials, the phonon and electron transport is forced to be along the a-axis and cannot be simply interpreted using the isotropic diffusion model. This physics can be used to explain the strong linear coherency between electrical and thermal conductivities of carbon-based structured materials. Also this strong anisotropy should be strictly considered when modeling the thermal conductivity of many carbon-based materials (e.g. those used in nuclear reactors) that are made of many small graphite grains with randomly oriented c-axis. Although various models have been developed in the past to correlate the thermal conductivity of composite materials with the structure and intrinsic thermal conductivity of the constituents [69], extremely strong thermal conductivity anisotropy has not been considered. This is also even critical for just pure carbon materials. So future work in this direction is urgently needed and will have profound and long-term impact. For the anisotropic temperature model, one good way is to use MD modeling to study the energy coupling, anisotropic specific heat, and thermal conductivity while experimental work is more challenging. Carbon-based nanomaterials in fact represent a very complicated category of structured materials. Its thermal conductivity, structural effects and temperature effects should be investigated with the extremely strong anisotropy in mind. The thermal reffusivity physical model provides a more advanced way to analyze the structural and temperature effects. This is also true for other materials' energy transport, either by phonons or electrons.

Declaration of Competing Interest

The authors declare that they have no known competing financial interests or personal relationships that could have appeared to influence the work reported in this paper.

Acknowledgments

This work was supported by the National Natural Science Foundation of China (52276080 for Y.X) and US National Science Foundation (CBET1930866 and CMMI2032464 for X.W).

References

- [1] Z.C. Wu, Z.H. Chen, X. Du, J.M. Logan, J. Sippel, M. Nikolou, K. Kamaras, J.R. Reynolds, D.B. Tanner, A.F. Hebard, A.G. Rinzler, Transparent, conductive carbon nanotube films, *Science* 305 (2004) 1273–1276, <https://doi.org/10.1126/science.1101243>
- [2] J. Zaumseil, Single-walled carbon nanotube networks for flexible and printed electronics, *Semicond. Sci. Technol.* 30 (2015) 074001, <https://doi.org/10.1088/0268-1242/30/7/074001>

- [3] A.A. Balandin, S. Ghosh, W.Z. Bao, I. Calizo, D. Teweldebrhan, F. Miao, C.N. Lau, Superior thermal conductivity of single-layer graphene, *Nano Lett.* 8 (2008) 902–907, <https://doi.org/10.1021/Nl0731872>
- [4] H.Y. Sun, Z. Xu, C. Gao, Multifunctional, ultra-flyweight, synergistically assembled carbon aerogels, *Adv. Mater.* 25 (2013) 2554–2560, <https://doi.org/10.1002/adma.201204576>
- [5] J. Yang, E.W. Zhang, X.F. Li, Y.T. Zhang, J. Qu, Z.Z. Yu, Cellulose/graphene aerogel supported phase change composites with high thermal conductivity and good shape stability for thermal energy storage, *Carbon* 98 (2016) 50–57, <https://doi.org/10.1016/j.carbon.2015.10.082>
- [6] D.P. Dong, H.T. Guo, G.Y. Li, L.F. Yan, X.T. Zhang, W.H. Song, Assembling hollow carbon sphere-graphene polyolithic aerogels for thermoelectric cells, *Nano Energy* 39 (2017) 470–477, <https://doi.org/10.1016/j.nanoen.2017.07.029>
- [7] Y. Fu, G. Wang, X. Ming, X.H. Liu, B.F. Hou, T. Mei, J.H. Li, J.Y. Wang, X.B. Wang, Oxygen plasma treated graphene aerogel as a solar absorber for rapid and efficient solar steam generation, *Carbon* 130 (2018) 250–256, <https://doi.org/10.1016/j.carbon.2017.12.124>
- [8] Y. Xie, M. Han, R. Wang, H. Zobeiri, X. Deng, P. Zhang, X. Wang, Graphene aerogel based bolometer for ultrasensitive sensing from ultraviolet to far-infrared, *ACS Nano* 13 (2019) 5385–5396, <https://doi.org/10.1021/acs.nano.9b00031>
- [9] G.H. Lee, D.K. Eftov, W. Jung, L. Ranzani, E.D. Walsh, T.A. Ohki, T. Taniguchi, K. Watanabe, P. Kim, D. Englund, K.C. Fong, Graphene-based Josephson junction microwave bolometer, *Nature* 586 (2020) 42–46, <https://doi.org/10.1038/s41586-020-2752-4>
- [10] M. Zhang, J.T.W. Yeow, Flexible polymer-carbon nanotube composite with high-response stability for wearable thermal imaging, *ACS Appl. Mater. Interfaces* 10 (2018) 26604–26609, <https://doi.org/10.1021/acsami.8b06482>
- [11] S. Si, W. Li, X. Zhao, M. Han, Y. Yue, W. Wu, S. Guo, X. Zhang, Z. Dai, X. Wang, X. Xiao, C. Jiang, Significant radiation tolerance and moderate reduction in thermal transport of a tungsten nanofilm by inserting monolayer graphene, *Adv. Mater.* 29 (2017) 17.
- [12] Y. Wang, D.H. Hurlley, E.P. Luther, M.F. Beaux, D.R. Vodnik, R.J. Peterson, B.L. Bennett, I.O. Usov, P. Yuan, X. Wang, M. Khafizov, Characterization of ultralow thermal conductivity in anisotropic pyrolytic carbon coating for thermal management applications, *Carbon* 129 (2018) 476–485, <https://doi.org/10.1016/j.carbon.2017.12.041>
- [13] X.X. Guo, S.J. Cheng, W.W. Cai, Y.F. Zhang, X.A. Zhang, A review of carbon-based thermal interface materials: Mechanism, thermal measurements and thermal properties, *Mater. Des.* 209 (2021), <https://doi.org/10.1016/j.matdes.2021.109936>
- [14] J. Khan, S.A. Momin, M. Mariatti, A review on advanced carbon-based thermal interface materials for electronic devices, *Carbon* 168 (2020) 65–112, <https://doi.org/10.1016/j.carbon.2020.06.012>
- [15] W. Yu, C.H. Liu, S.S. Fan, Advances of cnt-based systems in thermal management, *Nano Res.* 14 (2021) 2471–2490, <https://doi.org/10.1007/s12274-020-3255-1>
- [16] R. Bahru, N. Shaari, M.A. Mohamed, Allotrope carbon materials in thermal interface materials and fuel cell applications: a review, *Int J. Energ. Res* 44 (2020) 2471–2498, <https://doi.org/10.1002/er.5077>
- [17] W.X. Xiao, P. Wang, X.R. Song, B. Liao, K.Q. Yan, J.J. Zhang, Facile fabrication of anisotropic chitosan aerogel with hydrophobicity and thermal superinsulation for advanced thermal management, *ACS Sustain Chem. Eng.* 9 (2021) 9348–9357, <https://doi.org/10.1021/acssuschemeng.1c02217>
- [18] M.L. Zhang, S. Jiang, F.Y. Han, M.M. Li, N. Wang, L.F. Liu, Anisotropic cellulose nanofiber/chitosan aerogel with thermal management and oil absorption properties, *Carbohydr. Polym.* 264 (2021), <https://doi.org/10.1016/j.carbpol.2021.118033>
- [19] S.S. Chen, Q.Z. Wu, C. Mishra, J.Y. Kang, H.J. Zhang, K.J. Cho, W.W. Cai, A.A. Balandin, R.S. Ruoff, Thermal conductivity of isotopically modified graphene, *Nat. Mater.* 11 (2012) 203–207, <https://doi.org/10.1038/Nmat3207>
- [20] X.F. Xu, L.F.C. Pereira, Y. Wang, J. Wu, K.W. Zhang, X.M. Zhao, S. Bae, C.T. Bui, R.G. Xie, J.T.L. Thong, B.H. Hong, K.P. Loh, D. Donadio, B.W. Li, B. Ozyilmaz, Length-dependent thermal conductivity in suspended single-layer graphene, *Nat. Commun.* 5 (2014), <https://doi.org/10.1038/ncomms4689>
- [21] E. Pop, D. Mann, Q. Wang, K. Goodson, H. Dai, Thermal conductance of an individual single-wall carbon nanotube above room temperature, *Nano Lett.* 6 (2006) 96–100, <https://doi.org/10.1021/nl052145f>
- [22] M. Fujii, X. Zhang, H. Xie, H. Ago, K. Takahashi, T. Ikuta, H. Abe, T. Shimizu, Measuring the thermal conductivity of a single carbon nanotube, *Phys. Rev. Lett.* 95 (2005) 065502, <https://doi.org/10.1103/PhysRevLett.95.065502>
- [23] C.H. Yu, L. Shi, Z. Yao, D.Y. Li, A. Majumdar, Thermal conductance and thermo-power of an individual single-wall carbon nanotube, *Nano Lett.* 5 (2005) 1842–1846, <https://doi.org/10.1021/nl051044e>
- [24] M. Bauer, Q. Pham, C. Saltonstall, P. Norris, Thermal conductivity of vertically aligned carbon nanotube arrays: Growth conditions and tube inhomogeneity, *2608-1243, Appl. Phys. Lett.* 105 (2014), <https://doi.org/10.1063/1.4898708>
- [25] W. Yi, L. Lu, D.L. Zhang, Z.W. Pan, S.S. Xie, Linear specific heat of carbon nanotubes, *Phys. Rev. B* 59 (1999) R9015–R9018, <https://doi.org/10.1103/PhysRevB.59.R9015>
- [26] X.P. Huang, J.M. Wang, G. Eres, X.W. Wang, Thermophysical properties of multi-wall carbon nanotube bundles at elevated temperatures up to 830 k, *Carbon* 49 (2011) 1680–1691, <https://doi.org/10.1016/j.carbon.2010.12.053>
- [27] D.J. Yang, Q. Zhang, G. Chen, S.F. Yoon, J. Ahn, S.G. Wang, Q. Zhou, Q. Wang, J.Q. Li, Thermal conductivity of multiwalled carbon nanotubes, *Phys. Rev. B* 66 (2002) 165440, <https://doi.org/10.1103/PhysRevB.66.165440>
- [28] M.T. Pettes, H.X. Ji, R.S. Ruoff, L. Shi, Thermal transport in three-dimensional foam architectures of few-layer graphene and ultrathin graphite, *Nano Lett.* 12 (2012) 2959–2964, <https://doi.org/10.1021/nl300662g>
- [29] B. Wicklein, A. Kocjan, G. Salazar-Alvarez, F. Carosio, G. Camino, M. Antonietti, L. Bergstrom, Thermally insulating and fire-retardant lightweight anisotropic foams based on nanocellulose and graphene oxide, *Nat. Nanotechnol.* 10 (2015) 277–283, <https://doi.org/10.1038/Nnano.2014.248>
- [30] Y.S. Xie, S. Xu, Z.L. Xu, H.C. Wu, C. Deng, X.W. Wang, Interface-mediated extremely low thermal conductivity of graphene aerogel, *Carbon* 98 (2016) 381–390, <https://doi.org/10.1016/j.carbon.2015.11.033>
- [31] L. Spanu, S. Sorella, G. Galli, Nature and strength of interlayer binding in graphite, *Phys. Rev. Lett.* 103 (2009) 196401, <https://doi.org/10.1103/PhysRevLett.103.196401>
- [32] X. Chen, F. Tian, C. Persson, W. Duan, N.-X. Chen, Interlayer interactions in graphites, *Sci. Rep.* 3 (2013) 3046, <https://doi.org/10.1038/srep03046>
- [33] G.A. Slack, Anisotropic thermal conductivity of pyrolytic graphite, *Phys. Rev.* 127 (1962) 694–701, <https://doi.org/10.1103/PhysRev.127.694>
- [34] R. Taylor, The thermal conductivity of pyrolytic graphite, *Philos. Mag.: J. Theor. Exp. Appl. Phys.* 13 (1966) 157–166, <https://doi.org/10.1080/14786436608211993>
- [35] J.Q. Guo, X.W. Wang, T. Wang, Thermal characterization of microscale conductive and nonconductive wires using transient electrothermal technique, *J. Appl. Phys.* 101 (2007) 063537, <https://doi.org/10.1063/1.2714679>
- [36] T. Wang, X. Wang, J. Guo, Z. Luo, K. Cen, Characterization of thermal diffusivity of micro/nanoscale wires by transient photo-electro-thermal technique, *Appl. Phys. A* 87 (2007) 599–605, <https://doi.org/10.1007/s00339-007-3879-y>
- [37] J. Guo, X. Wang, D.B. Geohegan, G. Eres, Cc Vincent, Development of pulsed laser-assisted thermal relaxation technique for thermal characterization of microscale wires, *J. Appl. Phys.* 103 (2008) 113505, <https://doi.org/10.1063/1.2936873>
- [38] X.H. Feng, G.Q. Liu, S. Xu, H. Lin, X.W. Wang, 3-dimensional anisotropic thermal transport in microscale poly(3-hexylthiophene) thin films, *Polymer* 54 (2013) 1887–1895, <https://doi.org/10.1016/j.polymer.2013.01.038>
- [39] S. Xu, T. Wang, D. Hurlley, Y. Yue, X. Wang, Development of time-domain differential raman for transient thermal probing of materials, *Opt. Express* 23 (2015) 10040–10056.
- [40] C. Li, S. Xu, Y. Yue, B. Yang, X. Wang, Thermal characterization of carbon nanotube fiber by time-domain differential raman, *Carbon* 103 (2016) 101–108, <https://doi.org/10.1016/j.carbon.2016.03.003>
- [41] T. Wang, S. Xu, D.H. Hurlley, Y. Yue, X. Wang, Frequency-resolved raman for transient thermal probing and thermal diffusivity measurement, *Opt. Lett.* 41 (2016) 80–83.
- [42] P. Yuan, J. Liu, R. Wang, X. Wang, The hot carrier diffusion coefficient of sub-10 nm virgin mos₂: Uncovered by non-contact optical probing, *Nanoscale* 9 (2017) 6808.
- [43] P. Yuan, H. Tan, R. Wang, T. Wang, X. Wang, Very fast hot carrier diffusion in unconstrained mos₂ on a glass substrate: Discovered by picosecond et-raman, *RSC Adv.* 8 (2018) 12767–12778, <https://doi.org/10.1039/c8ra01106k>
- [44] P. Yuan, R. Wang, H. Tan, T. Wang, X. Wang, Energy transport state resolved raman for probing interface energy transport and hot carrier diffusion in few-layered mos₂, *ACS Photonics* 4 (2017) 3115–3129, <https://doi.org/10.1021/acsp Photonics.7b00815>
- [45] Y. Xie, Y. Yue, X. Wang, Part ii: Experimental methods to investigate heat transfer in nanoscale, in: Dimitrios Papavassiliou, Hai Duong, F. Gong (Eds.), *Thermal behaviour and applications of carbon-based nanomaterials*, Elsevier, 2020.
- [46] S.H. Simon, *The oxford solid state basics*, OUP, Oxford, 2013.
- [47] H.E. Jackson, C.T. Walker, Thermal conductivity, second sound, and phonon-phonon interactions in naf, *Phys. Rev. B* 3 (1971) 1428, <https://doi.org/10.1103/PhysRevB.3.1428>
- [48] H.E. Jackson, C.T. Walker, T.F. Mcnelli, Second sound in naf, *Phys. Rev. Lett.* 25 (1970) 26, <https://doi.org/10.1103/PhysRevLett.25.26>
- [49] C.Y. Ho, R.W. Powell, P.E. Liley, Thermal conductivity of the elements: A comprehensive review iii American Chemical Society, Washington, 1975, p. 796.
- [50] S.S. Chen, A.L. Moore, W.W. Cai, J.W. Suk, J.H. An, C. Mishra, C. Amos, C.W. Magnuson, J.Y. Kang, L. Shi, R.S. Ruoff, Raman measurements of thermal transport in suspended monolayer graphene of variable sizes in vacuum and gaseous environments, *ACS Nano* 5 (2011) 321–328, <https://doi.org/10.1021/Nn102915x>
- [51] Y. Xie, Z. Xu, S. Xu, Z. Cheng, N. Hashemi, C. Deng, X. Wang, The defect level and ideal thermal conductivity of graphene uncovered by residual thermal reffusivity at the 0 k limit, *Nanoscale* 7 (2015) 10101–10110, <https://doi.org/10.1039/c5nr02012c>
- [52] Y. Xie, B. Zhu, J. Liu, X.U. ZaoLi, X. Wang, Thermal reffusivity: Uncovering phonon behavior, structural defects, and domain size, *Front. Energy* 12 (2018) 143–157, <https://doi.org/10.1007/s11708-018-0520-z>
- [53] Z.L. Xu, X.W. Wang, H.Q. Xie, Promoted electron transport and sustained phonon transport by DNA down to 10 k, *Polymer* 55 (2014) 6373–6380, <https://doi.org/10.1016/j.polymer.2014.10.016>
- [54] P.M. Charles Kittel, S. Johnson (Ed.), *Introduction to solid state physics*, 8th ed., John Wiley & Sons, Inc., 2005.
- [55] K.A. Denault, J. Brgoch, S.D. Kloss, M.W. Gaultois, J. Siewenie, K. Page, R. Seshadri, Average and local structure, debye temperature, and structural rigidity in some oxide compounds related to phosphor hosts, *ACS Appl. Mater. Interfaces* 7 (2015) 7264–7272, <https://doi.org/10.1021/acsami.5b00445>
- [56] C.H. Deng, Y.M. Sun, L.J. Pan, T.Y. Wang, Y.S. Xie, J. Liu, B.W. Zhu, X.W. Wang, Thermal diffusivity of a single carbon nanocil: uncovering the correlation with temperature and domain size, *ACS Nano* 10 (2016) 9710–9719, <https://doi.org/10.1021/acsnano.6b05715>
- [57] Y.S. Xie, P.Y. Yuan, T.Y. Wang, N. Hashemi, X.W. Wang, Switch on the high thermal conductivity of graphene paper, *Nanoscale* 8 (2016) 17581–17597, <https://doi.org/10.1039/c6nr06402g>
- [58] J. Liu, W.D. Qu, Y.S. Xie, B.W. Zhu, T.Y. Wang, X.L. Bai, X.W. Wang, Thermal conductivity and annealing effect on structure of lignin-based microscale carbon fibers, *Carbon* 121 (2017) 35–47, <https://doi.org/10.1016/j.carbon.2017.05.066>

- [59] Y.A. Yue, K. Liu, M. Li, X.J. Hu, Thermal manipulation of carbon nanotube fiber by mechanical stretching, *Carbon* 77 (2014) 973–979, <https://doi.org/10.1016/j.carbon.2014.06.013>
- [60] H. Hu, Z.B. Zhao, W.B. Wan, Y. Gogotsi, J.S. Qiu, Ultralight and highly compressible graphene aerogels, *Adv. Mater.* 25 (2013) 2219–2223, <https://doi.org/10.1002/adma.201204530>
- [61] N. Hunter, A. Karamati, Y.S. Xie, H. Lin, X.W. Wang, Laser photoreduction of graphene aerogel microfibers: Dynamic electrical and thermal behaviors, *Chemphyschem* 23 (2022) ARTN e202200417 [10.1002/cphc.202200417](https://doi.org/10.1002/cphc.202200417).
- [62] N.H. Huan Lin, Hamidreza Zobeiri, Yanan Yue, Xinwei Wang, Ultra-high thermal sensitivity of graphene microfiber, *Carbon* 203 (2023) 620–629, <https://doi.org/10.1016/j.carbon.2022.12.013>
- [63] M. Han, J. Liu, Y. Xie, X. Wang, Sub- μm c-axis structural domain size of graphene paper uncovered by low-momentum phonon scattering, *Carbon* 126 (2018) 532–543, <https://doi.org/10.1016/j.carbon.2017.10.070>
- [64] C. Deng, C. Li, P. Wang, X. Wang, L. Pan, Revealing the linear relationship between electrical, thermal, mechanical and structural properties of carbon nanocoils, *Phys. Chem. Chem. Phys.* 20 (2018) 13316–13321, <https://doi.org/10.1039/c8cp01349g>
- [65] C. Deng, T. Cong, Y. Xie, R. Wang, T. Wang, L. Pan, X. Wang, In situ investigation of annealing effect on thermophysical properties of single carbon nanocoil, *Int. J. Heat. Mass Transf.* 151 (2020) 119416, <https://doi.org/10.1016/j.ijheatmasstransfer.2020.119416>
- [66] J. Gao, H. Zobeiri, H. Lin, D. Xie, Y. Yue, X. Wang, Coherency between thermal and electrical transport of partly reduced graphene paper, *Carbon* 178 (2021) 92–102, <https://doi.org/10.1016/j.carbon.2021.02.102>
- [67] J. Liu, T. Wang, S. Xu, P. Yuan, X. Xu, X. Wang, Thermal conductivity of giant mono- to few-layered cvd graphene supported on an organic substrate, *Nanoscale* 8 (2016) 10298–10309, <https://doi.org/10.1039/c6nr02258h>
- [68] A.K. Dutta, Electrical conductivity of single crystals of graphite, *Phys. Rev.* 90 (1953) 187–192, <https://doi.org/10.1103/PhysRev.90.187>
- [69] X. Wang, X. Xu, S.U.S. Choi, Thermal conductivity of nanoparticle - fluid mixture, *J. Thermophys. Heat. Transf.* 13 (1999) 474–480, <https://doi.org/10.2514/2.6486>

Dr. Yangsu Xie is an associate professor at Shenzhen University, China. She obtained her Ph.D. from Iowa State University in 2017, B.S. from Huazhong University of Science and Technology in 2013. Since here Ph.D. study, she has devoted into studying the thermal and electrical transport behaviors of carbon-based nanomaterials at low temperatures and the underlying phonon scattering mechanisms. Her work uncovers the significant effect of structural defects, interfaces, and thermal strain on the thermal and electrical properties of carbon-based nanomaterials.

Dr. Xinwei Wang is the Anson Marston Distinguished Professor at Iowa State University. He obtained his Ph.D. from Purdue University in 2001, M.S. (1996) and B.S. (1994) from the University of Science and Technology of China. Over the past 20 years, he has led his laboratory to develop new techniques for measuring thermophysical properties at the micro/nanoscale and investigate the structural effects. Some of his noted works include the first time distinguishing optical and acoustic phonon temperatures, conjugated phonon and hot carrier transport, and radiative electron-hole recombination, as well as the thermal reffusivity theory for characterizing energy carrier scattering by structures.